ACS APPLIED MATERIALS & INTERFACES

Research Article

www.acsami.org

Cellulose Nanofiber Orientation in Nanopaper and Nanocomposites by Cold Drawing

Houssine Sehaqui,*[,†] Ngesa Ezekiel Mushi,[†] Seira Morimune,[‡] Michaela Salajkova,[§] Takashi Nishino,[‡] and Lars A. Berglund[†,§]

[†]Department of Fibre and Polymer Technology and [§]Wallenberg Wood Science Center, Royal Institute of Technology, SE-100 44 Stockholm, Sweden,

[‡]Department of Chemical Science and Engineering, Kobe University, Kobe 657-8501, Japan

ABSTRACT: To exploit the mechanical potential of native cellulose fibrils, we report on the preparation of nanopaper with preferred orientation of nanofibrillated cellulose (TEMPO-NFC) by cold drawing. The preparation route is papermaking-like and includes vacuum filtering of a TEMPO-oxidated NFC water dispersion, drawing in wet state and drying. The orientation of the fibrils in the nanopaper was assessed by AFM and wide-angle X-ray diffraction analysis, and the effect on mechanical properties of the resulting nanopaper structure was investigated by tensile tests. At high draw ratio, the degree of orientation is as high as 82 and 89% in-the-plane and cross-sectional planes of the nanopaper, respectively, and the Young's modulus is 33 GPa. This is much higher than mechanical properties of isotropic nanopaper. The cold drawing method can be also applied to NFC nanocomposites as demonstrated by preparation of TEMPO-NFC/hydroxyethyl cellulose (HEC) nanocomposites. The introduction of the soft HEC matrix allows further tailoring of the mechanical properties.

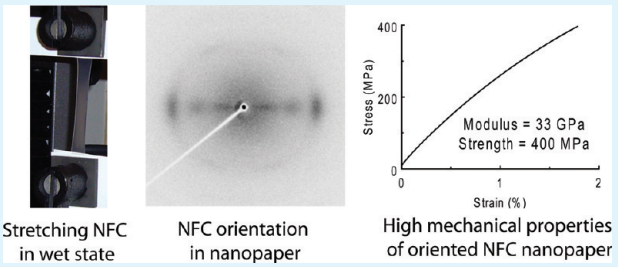

KEYWORDS: *nanopaper, cellulose nanofibers, orientation, cold drawing, nanocomposites, nanofibrillated cellulose*

INTRODUCTION

Nanofibrillated cellulose (NFC) refers to individual microfibrils or cellulose microfibril aggregates disintegrated from the plant cell wall of cellulose sources such as wood pulp fibers. NFC nanofibers are few micrometers long with a typical lateral dimension in the 5−20 nm range. NFC were first produced in 1983 by Turbak et al. They subjected a wood pulp slurry to high mechanical forces in a homogenizer.[1] This led to the disintegration of 25−100 nm nanofibrils into an aqueous dispersion. Nowadays, disintegration of NFC is facilitated: the use of enzymatic[2,3] or chemical pretreatment[4] lowers the energy required for the disintegration process and leads to smaller diameter of the nanofibrils (5−20 and 5 nm, respectively). Furthermore, other equipments and methods for mechanical disintegration are currently available including homogenizer,[1] microfluidizer,[5,6] grinder,[7] blender,[8] and sonicator.[8,9] Even simple mechanical stirring of chemically pretreated (TEMPO oxidized) wood pulp fibers can disintegrate them.[8] TEMPO-mediated oxidation of cellulosic fibers introduces negatively charged carboxyl groups on the fibril surface and the repulsive forces between charged fibrils facilitate the disintegration process. Other advantages include preservation of cellulose I crystalline structure of native cellulose in the interior of the fibrils, and the lateral dimension is typically 4−5 nm, which corresponds to the smallest fibrils present in the plant cell wall.

NFC-based materials are from renewable resources, are biodegradable and the cellulose crystal has high axial modulus (~150 GPa),[10] and NFC has strong network forming characteristics.[11] Furthermore, pretreated wood pulp can be disintegrated at low cost. Initially, aqueous NFC dispersions were used as rheological modifiers for applications in food, cosmetics and chemical products.[1] More recently, NFC from wood pulp has become an important material building block. NFC has been used for nanopaper,[5,12] foams[13,14] and aerogels,[15,16] and as reinforcement in a range of polymer matrices.[17−19] NFC has also been used as a substrate for functional materials including electrically conductive all-polymer batteries,[20] magnetic nanopaper,[21] and transparent and foldable films for display applications.[22] Although these NFC materials have good mechanical properties, the full mechanical potential of NFC was not fully achieved because the orientation distribution of NFC was random-in-the-plane or random-in-space.

Several efforts to orient cellulose nanofibers and whiskers have been presented. Orientation has been reported in dispersions, films, and fibers. In a dispersion, cellulose microcrystals undergo spontaneous parallel arrangements in the form of a chiral nematic phase.[23] A magnetic[24] or electric[25] field can also orientate rodlike cellulose whiskers in the liquid state, and subsequent drying gives oriented films. Films of highly oriented cellulose whiskers have been reported by

Received: November 29, 2011
Accepted: January 18, 2012
Published: January 18, 2012

rotation of a glass vial containing aqueous dispersion of whiskers, followed by drying.[26] All-cellulose films (composite films of cellulose I and II) were cold drawn in the wet state to induce orientation in the drawing direction.[27] For fibers with oriented cellulose, wet spinning, hot drawing and electrospinning have been used. Wet spinning has been used on wood cellulose nanofiber and tunicate whisker dispersions using acetone as a coagulation bath. The spinning rate and the nature of the starting dispersion was found to give different fiber structure (hollow or porous fibers).[28] Hot-drawing in the presence of a polymer matrix was used to obtain fibers with cellulose whiskers in a PVA matrix where both the PVA matrix and the whiskers showed a high degree of orientation.[29] Electrospinning also gives fibers with oriented whiskers in a polymer matrix. The electrospun fibers can be randomly assembled into a porous membrane, or aligned with a drum collector.[30]

The starting point of the present study is NFC nanopaper, and this is a web-like network of cellulose nanofibrils.[5,12] The NFC orientation distribution is random-in-the-plane. Interesting properties include optical transparency,[31] smoothness,[12] low coefficient of thermal expansion,[31] good mechanical properties,[5,12] and possibilities for functionalization.[21,32] The nanopaper can be prepared by a water-based papermaking-like filtration procedure,[5,12] and therefore offers solvent-free preparation compared with regenerated cellulose films. Furthermore, the nanopaper consists of cellulose I type fibrils with better mechanical properties compared to cellulose II.[33] Suggested applications for NFC nanopaper includes films for packaging applications,[5,6] electronic display application[22] or as a substrate for nanocomposites preparation (e.g., by impregnation).[34] In this later application, an advantage would be to have orientation of NFC so that further tailoring of the mechanical properties becomes possible. For instance, it would be possible to prepare laminates based on oriented film "plies" stacked with varying orientation angle so that mechanical properties in different directions can be tailored.

Cold drawing has already been used for preparation of all-cellulose films with preferred orientation.[27] The preparation steps of oriented all-cellulose films include partial dissolution of MCC in LiCl-DMAc solvent, gelation, washing, drying of the films, wetting of the dried films, stretching (cold drawing) of the wet films, and finally drying the films in stretched conditions. The drawn all-cellulose films presented excellent mechanical properties and the advantage of cold drawing was clearly demonstrated.

The present paper is an attempt to orient TEMPO-NFC in the nanopaper by cold-drawing of the wet "hydrogel cake" resulting from filtration and containing 70−90% water. No organic solvent is used. A three-step papermaking route is used including vacuum filtration, hydrogel drawing and drying. Effects of drawing on fibril orientation and on mechanical properties of oriented nanopaper are evaluated. In the last part, we show the applicability of the drawing method for TEMPO-NFC based nanocomposites using hydroxyethyl cellulose (HEC) as a matrix. Effects of the polymer matrix on the mechanical properties of the drawn TEMPO-NFC nanocomposites are discussed. In a recent conference, independent work on oriented nanopaper was presented orally and as an abstract.[35] This paper additionally discusses the cold-drawing of TEMPO-NFC based composites.

EXPERIMENTAL SECTION

Disintegration of TEMPO-NFC. TEMPO-NFC aqueous dispersion was prepared from softwood sulphite pulp fibers (DP of 1200, lignin and hemicelluloses contents of 0.7% and 13.8%, respectively, Nordic Paper Seffle AB, Sweden) according to the TEMPO-mediated oxidation method reported by Saito et al.[8] The pulp was first dispersed in water in which sodium bromide and TEMPO were dissolved (1 and 0.1 mmol per gram of cellulose, respectively). The concentration of the pulp in water was 2 wt %. The reaction was started by addition of sodium hypochlorite (10 mmol per gram of cellulose) dropwise into the dispersion. During the addition of NaClO, carboxylate groups were forming on the surface of the fibrils and the pH decreased. The pH of the reaction was then maintained at 10 by sodium hydroxide addition (i.e., the pulp fibers in the salt form). After all NaClO was consumed, the pulp fibers were filtered and washed several times with deionized water until the filtrate solution was neutral. The purified pulp fibers were then dispersed in water at a concentration of 1 wt % and disintegrated by a homogenization process with a Microfluidizer M-110EH (Microfluidics Ind., USA). The carboxylate content of TEMPO-NFC determined by titration is 2.3 mmol g^{-1}.

Preparation of Reference TEMPO-NFC Nanopaper. Preparation of NFC Nanopaper was reported previously.[5] The 1 wt % TEMPO-NFC dispersion was diluted to 0.1% by water addition and stirring and subsequently degassed. The 0.1% TEMPO-NFC dispersion was vacuum filtered on a glass filter funnel (7.2 cm in diameter) using filter membrane, 0.65 μm DVPP, Millipore. After filtration, a wet "cake" is formed. The cake has a water content of 70−90% as determined on a series of cakes obtained after vacuum filtration using oven drying at 105 °C. This cake is peeled from the membrane and stacked first between two woven metal cloths and then two paper carrier boards. This package was placed in a sheet dryer (Rapid Köthen-Rycobelgroup) for 12 min at 93 °C and a vacuum of about 70 mbar. The resulting nanopaper had a thickness of ca. 50 μm.

Cold Drawn TEMPO-NFC Nanopaper with Partial Alignment of the Fibrils. The wet TEMPO-NFC cake is prepared as above. From the cake, 1 cm wide strips were cut, clamped on a tensile testing equipment (Instron 5944) and stretched at a tensile rate of 50% min^{-1} until the strain reached 20, 40, or 60% (corresponding to draw-ratio DR of 1.2, 1.4, and 1.6 respectively). The stretching was stopped, and the samples were taken in the stretched conformation, tapped into woven metal cloths and put between two paper carrier boards and dried as above.

Cold Drawn TEMPO-NFC/HEC Nanocomposite with Partial Alignment of the Fibrils. Hydroxyethyl cellulose, average $M_v \approx 1.3$ Mg/mol, substitution degree 1.5, molar substitution 2.5 ethylene oxide groups per anhydroglucose unit was purchased from Aldrich. HEC was dissolved in water and mixed with a 0.1 wt % TEMPO-NFC dispersion using magnetic stirring overnight. The amount of HEC and TEMPO-NFC were chosen to have 20 wt % HEC in the final composite (see ref 19 for more details on the preparation). The mixtures were degassed and then vacuum filtered on a glass filter funnel using a 0.65 μm filter membrane (DVPP, Millipore). The wet nanocomposite cake formed at the end of the filtration was taken, cut into strips, stretched, and dried as described above.

Field-Emission Scanning Electron Microscopy (FE-SEM). The TEMPO-NFC were dried using carbon dioxide supercritical drying and the procedure is explained in details elsewhere.[36] They were observed by SEM using a Hitachi S-4800 equipped with a cold field emission electron source. The samples were coated with graphite and gold−palladium using Creesington 208 HR sputter coaters (ca. 5 nm). Secondary electron detector was used for capturing images at 1 kV.

Light Transmittance. Regular light transmittance was measured using a UV−visible spectrophotometer (Cary 1E, Varian Corp.) by placing the specimens in the entrance port of the detection system. Percent transmittance at 200−800 nm was recorded.

Atomic Force Microscopy (AFM). Nanoscope IIIa AFM (Picoforce SPM, Veeco, Santa Barbara, CA) was used to view surface micrographs of TEMPO-NFC nanopapers. All measurements were performed in the tapping mode with a scan rate of 2 Hz/512 dots using standard noncontact silicon cantilevers (RTESP, Veeco, Santa

Barbara, CA) with a tip radius of 8 nm and a spring constant of 40 N/m. The micrographs were taken from the amplitude images over a 0.5 × 0.5 μm^2 area. No image processing except flattening was undertaken.

X-ray Diffraction. Wide angle X-ray diffraction photographs were obtained by irradiating the sample by Cu Kα radiation in the direction both perpendicular (in-the-plane) and parallel (cross-section) to the nanopaper surface. From azimutal intensity distribution graphs for the 200 equatorial reflection (most intense peak), two kinds of orientation factors, namely the degree of orientation (Π), and Hermans orientation parameter (f), were calculated according to eqs 1−3. The Herman's orientation parameter describes the extent of orientation of cellulose crystalites axis relative to other axis of interest (in this case the axis of drawing). fwhm is the full width at half-maximum. Φ represents the azimuthal angle (angle between the axis of drawing and cellulose crystallites axis) and $I(\Phi)$ is the intensity along the Debye−Scherrer ring. $f = 1$ corresponds to a maximum orientation parallel to the drawing direction, whereas $f = 0$ indicates random orientation of the fibrils.

$$\Pi = \frac{180 - FWHM}{180} \quad (1)$$

$$f = \frac{3\langle \cos^2 \varphi \rangle - 1}{2} \quad (2)$$

$$\langle \cos^2 \varphi \rangle = \frac{\sum_0^{\pi/2} I(\varphi) \sin \varphi \cos^2 \varphi}{\sum_0^{\pi/2} I(\varphi) \sin \varphi} \quad (3)$$

Mechanical Properties. Tensile tests on TEMPO-NFC nanopapers were performed using an Instron universal materials testing machine equipped with a 500 N load cell. Reference and drawn specimen strips were conditioned overnight at 50% relative humidity and 23 °C and tested under these conditions by having a gauge length distance of ca. 20 mm and by using a tensile strain rate of 5% min^{-1}. Young's modulus was determined as the slope at low strain, the tensile strength was determined as the stress at specimen breakage. Three samples were tested for the DR = 1 and DR = 1.2, two samples were tested for the DR = 1.4, and one sample was tested for the DR = 1.6. The lack of samples for high DR is due to premature breakage of the TEMPO-NFC cake during stretching.

RESULTS AND DISCUSSION

Characterization of TEMPO-NFC. TEMPO-NFC aqueous dispersions were successfully prepared based on TEMPO oxidized wood pulp fibers followed by one pass through a microfluidizer. Drying of the dispersion by supercritical drying allows the preservation of the fibrillar structure for SEM observation (Figure 1). Visual observations provide estimates of

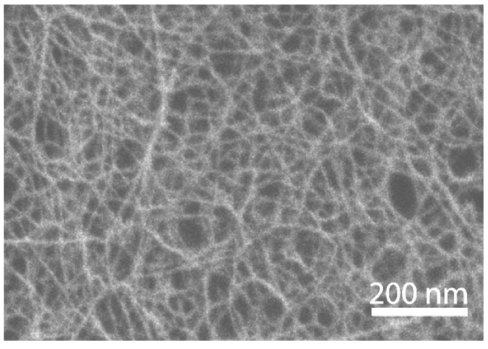

Figure 1. SEM micrograph of TEMPO-NFC.

the TEMPO-NFC diameter to be 5−10 nm, and the length to be at least of 500 nm. The true diameter of the fibrils is expected to be smaller than 10 nm, because a coating was applied to the fibrils for SEM observation. In our previous study,[36] the diameter of TEMPO-NFC disintegrated from wood fibers was calculated from the surface area of the fibrillar aerogel network and found to be of 5.7 nm assuming a cylindrical shape of the fibrils. These observations confirm that microfibrils (plant physiology term for smallest cellulose fibril) were successfully disintegrated from wood pulp fibers by TEMPO pretreatment.

Using vacuum filtration of TEMPO-NFC dispersion, TEMPO-NFC nanopaper of 72 mm in diameter was prepared. In a previous study,[12] we extended this method in a laboratory papersheet former (Rapid-Köthen) to prepare 200 mm large NFC nanopaper sheets and clay/NFC hybrid nanopaper sheets. NFC prepared by the enzymatic method was used, it had a diameter of 5−20 nm and the corresponding nanopaper presented smoothness and optical transparency (light transmittance of ca. 50% at 600 nm).[12] In the present study, the fibrils are smaller in diameter due to the different TEMPO-NFC preparation route. Consequently, the optical transparency of the TEMPO-NFC nanopaper is as high as 80% at 600 nm as observed in Figure 2.

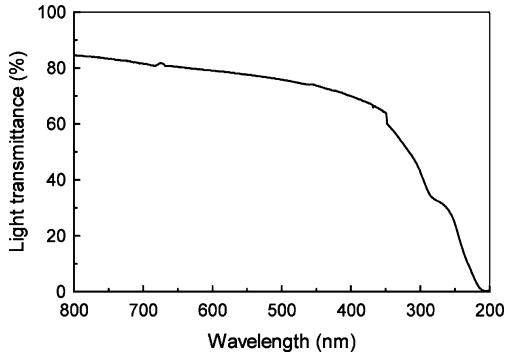

Figure 2. Light transmittance vs wavelength of TEMPO-NFC nanopaper.

Drawing of TEMPO-NFC. Since the nanopaper structures studied so far are characterized by random-in-the-plane orientation of the NFC,[5] the stiffness potential is not fully utilized. Attempts to partially orient NFC have been reported using the dynamic sheet former,[37] but low modulus and strength were obtained. Furthermore, there was loss of the fibrils through the membrane during the preparation process.

After vacuum filtration of the TEMPO-NFC aqueous dispersion, a TEMPO-NFC cake is formed (see Figure 3). Although the cake has a water content of 70−90%, it is mechanically robust. It is expected that the high aspect ratio of the fibrils combined with their high specific surface area result in entanglement of the fibrils in the cake which lead to the mechanical stability of the cake. Furthermore, attractive interactions between the fibrils such as hydrogen bonds and Van der Waals forces may also add strength to the cake. Moreover, the cake can be stretched up to 60% prior to rupture, which is far above the strain to failure of dry nanopapers that is in the 5−10% range.[5,12] The reasons are in the weakening of interfibril interactions compared with the dry state, which facilitates drawing. Desorption of water during drying increases molecular interfibril interaction and therefore the structure is arrested in a state of preferred orientation.

Compared to wet all-cellulose films drawn to 50%,[27] the TEMPO-NFC cake has slightly higher drawability (60%). The

Figure 3. TEMPO-NFC cake obtained after vacuum filtration of TEMPO-NFC aqueous dispersion (water content in the cake is 70–90%).

other advantage is that stretching can be performed in the never dried state, while fragility for all-cellulose gel in the never-dried state was reported. There was a need to dry all-cellulose films and rewet them in order to achieve elongation of 50%.

AFM. The surface of the dried TEMPO-NFC nanopaper was observed by AFM. In order to observe the effect of drawing, two samples were selected: a reference TEMPO-NFC nanopaper sample (DR = 1, Figure 4.a) and a drawn nanopaper

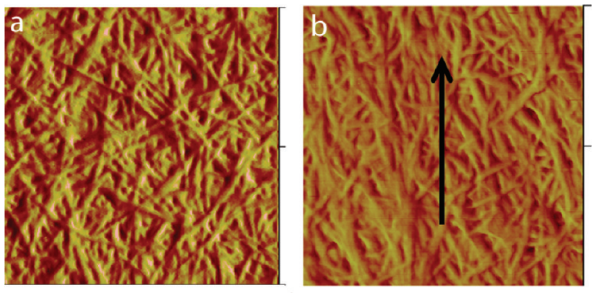

Figure 4. AFM micrographs of surfaces of (a) a reference nondrawn TEMPO-NFC nanopaper sample (DR = 1), (b) a drawn TEMPO-NFC nanopaper at DR = 1.4.

sample (DR = 1.4, Figure 4b). The scanned area is 0.5 × 0.5 μm^2. The reference nondrawn TEMPO-NFC nanopaper clearly shows a random in-the-plane orientation of the fibrils. The random orientation has been reported in other studies and results during the vacuum filtration step.[5] The drawn nanopaper shows preferred orientation of the fibrils parallel to the direction of drawing (arrow direction). The orientation of the fibrils occurs during drawing of the cake as shearing of the fibrils is induced.

XRD. XRD measurements were undertaken perpendicular and parallel to the plane of the nanopaper in order to assess orientation of the fibrils. Reference nonstretched TEMPO-NFC nanopaper sample (referred to as DR = 1), and drawn nanopapers of DR = 1.2 and DR = 1.6 were selected. XRD diffractograms are shown in Figure 5. When the beam is perpendicular to the nanopaper plane (in-plane direction

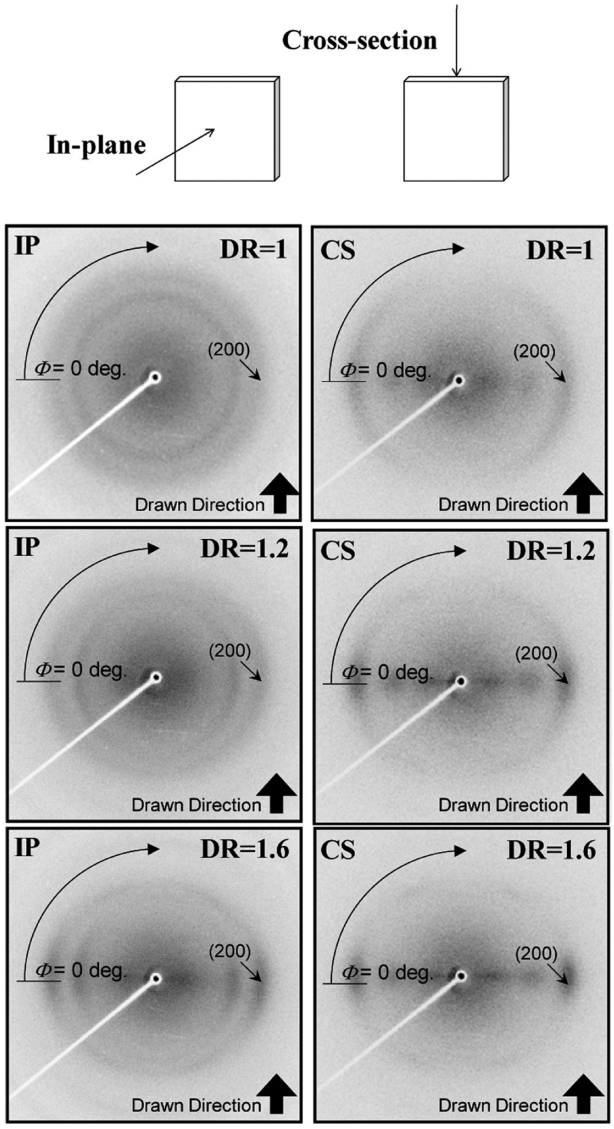

Figure 5. XRD patterns in the in-plane direction (IP) and cross-sectional direction (CS) of the non stretched TEMPO-NFC nanopaper reference sample (DR = 1), and the samples stretched at 20% (DR = 1.2) and 60% (DR = 1.6).

referred to as IP), ring patterns are observed for the reference nondrawn nanopaper, and this corresponds to random-in-the-plane distribution of the fibrils (in agreement with AFM picture in Figure 4a). By increasing the draw-ratio, equatorial arc patterns are formed as the cellulose crystallites are aligning in the drawing direction. Because the *c*-axis of cellulose crystals follow the TEMPO-NFC fiber axis, the cellulose crystallites represent the nanofiber orientation in the drawn nanopaper.

In the cross-sectional plane (CS), preferred orientation of the nonstretched TEMPO-NFC nanopaper can be observed in the XRD diffractogram. This implies that (200) was aligned parallel to the film surface and this occurs during vacuum filtration.[5] Increasing the draw ratio led to an increase in the fibrils orientation in the cross-sectional plane. At the highest draw-ratio, arc patterns are confined to spots suggesting a high degree of TEMPO-NFC orientation.

dx.doi.org/10.1021/am2016766 | *ACS Appl. Mater. Interfaces* 2012, 4, 1043–1049

The azimuthal profiles of the equatorial reflection (200) are presented in Figure 6. These plots allow quantification of

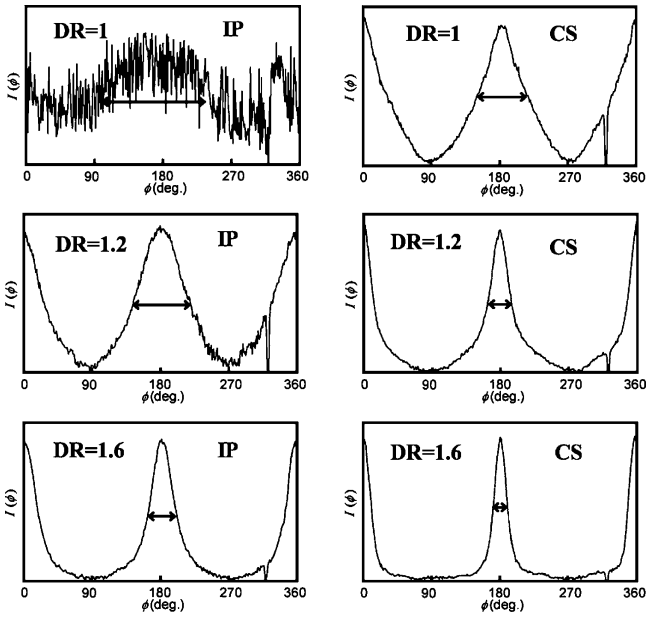

Figure 6. Azimuthal intensity distributions of the equatorial reflection (200) for the nonstretched TEMPO-NFC nanopaper reference sample (DR = 1), and the samples stretched at 20% (DR = 1.2). and 60% (DR = 1.6).

TEMPO-NFC orientation. Upon drawing, clear intensity maxima develop, indicating increasing preferred orientation of the TEMPO-NFC parallel to the draw direction. More narrow peaks are observed at high DR. From the full width at half-maximum (fwhm) of the peaks, the degree of orientation Π was calculated (eq 1). The results are presented in Table 1. At the

Table 1. Degree of Orientation (Π) and Hermans Orientation Parameter (f) of Nanopaper Samples

	fwhm (deg)		degree of orientation, Π (%)		Herman's orientation factor, f	
draw ratio	IP	CS	IP	CS	IP	CS
1	131	68	30.6	62.2	0.08	0.34
1.2	67	30	62.8	83.3	0.36	0.57
1.6	33	19	81.7	89.4	0.56	0.72

highest draw ratio, the degree of orientation (Π) is as high as 82% and 89% in-the-plane and cross-section plane, respectively. This is higher than reported for wet-spun fibers from wood cellulose nanofibers (Π between 0.65 and 0.72)[28] and is in the same order of alignment as for fibers of highly oriented cellulose whiskers in a PVA matrix (Π between 0.87 and 0.9).[29] The Herman's orientation factor f was also evaluated. As for the degree of orientation, f increases with increased draw-ratio. Values of f = 0.56 and f = 0.72 are found for the highest draw-ratio in-the-plane and cross-section respectively. These values are higher than reported for all-cellulose films (f = 0.29)[27] and lower than values for films of highly oriented cellulose microcrystals prepared by rotation on a drum (f = 0.96 for cladophora and f = 0.90 for ramie fibers).[26] The short aspect ratio of cellulose microcrystals facilitates orientation. The drawback is brittleness of the corresponding films.

Mechanical Properties. Mechanical properties of nanopaper with oriented nanofibrils were compared to reference nondrawn nanopaper. Tensile stress–strain curves are presented in Figure 7 and results are compiled in Table 2.

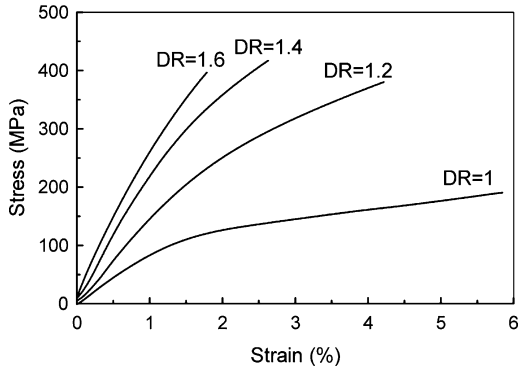

Figure 7. Tensile stress–strain curves of TEMPO-NFC nanopaper. Draw ratio is presented next to the curves.

Table 2. Tensile Properties of Drawn TEMPO-NFC Nanopaper

	draw ratio			
	1	1.2	1.4	1.6
modulus (GPa)	10.3 (0.8)	17.3 (4.0)	24.6 (0.4)	33.3
strength (MPa)	185 (7.7)	345 (40)	428 (15)	397
strain at break (%)	5.26 (0.56)	3.55 (1.21)	2.46 (0.23)	1.79

Stiffness and strength increases significantly with draw-ratio while the strain to failure considerably decreases. The reference nondrawn TEMPO-NFC nanopaper sample has a modulus of 10 GPa, a strength of 185 MPa and a strain to failure of 5.3%. These values agree with reported mechanical property data of NFC nanopaper.[5,12] At a draw-ratio of 1.2, the modulus increases to 17.3 GPa and the strength to 345 MPa. The modulus reaches a maximum of 33 GPa at DR = 1.6. At this DR, the strength is 400 MPa and the strain to failure 1.8%. The strength and modulus of drawn nanopaper are significantly improved compared with previously reported isotropic nanopaper films. A linear relationship was found between modulus and draw-ratio (see Figure 8). Such linear relationship was also

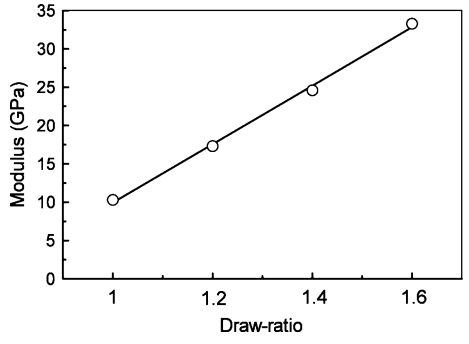

Figure 8. Modulus vs draw ratio for TEMPO-NFC nanopaper.

reported for drawing of all-cellulose films.[27] There is also a similarity between the mechanical properties of the present drawn TEMPO-NFC nanopaper and all-cellulose films (modulus increase from 10 to 33 GPa, strength increase from 200 to 430 MPa and strain to failure drops from 16.1 to 2.3%

dx.doi.org/10.1021/am2016766 | ACS Appl. Mater. Interfaces 2012, 4, 1043–1049

for drawn all-cellulose films). Comparing with data for wet-spun fibers made of cellulose nanofibers (modulus = 8.4−23.6 GPa, strength 90 - 332 MPa and strain to failure 1.5−3.1%),[28] the present nanopaper data are higher. This could be due to lower orientation of the fibrils and the hollow structure of the wet-spun fibers.[28] Compared to mechanical properties of highly oriented cellulose whiskers in PVA matrix prepared by hot drawing (modulus 42−56 GPa, strength 1320−1890 MPa and strain to failure 3.8−9.4%), the mechanical properties of the present nanopaper are considerably lower. This could be due to the high mechanical properties of the neat PVA matrix (degree of orientation as high as 0.97 and modulus of 30 GPa for the neat PVA matrix) and to the high orientation of the cellulose whiskers in the matrix (degree of orientation 0.87−0.9).

Cold Drawing of TEMPO-NFC/HEC Nanocomposites. In a previous study, we reported on mechanical properties of NFC/HEC nanocomposites.[19] The soft HEC matrix associated with and surrounding NFC was found to considerably increase the strain to failure of the composites and their toughness expressed as work to fracture (area under stress−strain curve) was remarkably high. In the present study, we draw TEMPO-NFC/HEC nanocomposites and investigate the effect of draw-ratio on mechnical properties. TEMPO-NFC was well dispersed into the HEC aqueous solution, the mixture was vacuum filtered and the nanocomposite "hydrogel cake" thus obtained (containing ca. 80% TEMPO-NFC and 20% HEC) was drawn. It was found that the nanocomposite cake can be stretched up to 80% strain before rupture. The higher draw-ratio possible compared to TEMPO-NFC "hydrogel cake" (stretching to max 60% strain) is due to the presence of ductile HEC. Upon drawing of the nanocomposite cake, TEMPO-NFC and HEC are aligned along the drawing direction. After drying the nanocomposite cake, mechanical properties of the obtained TEMPO-NFC/HEC nanocomposites were measured. Tensile stress−strain curve of TEMPO-NFC/HEC nanocomposites of draw-ratio of 1.8 are presented in Figure 9 and

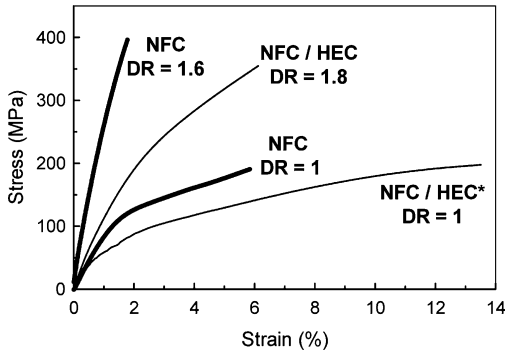

Figure 9. Tensile stress−strain curves of drawn TEMPO-NFC/HEC nanocomposites and reference materials. * data from ref 19 for nanocomposites of 68 wt % NFC and 32 wt % HEC.

compared to the drawn TEMPO-NFC nanopaper of DR = 1.6, to the reference nonstretched TEMPO-NFC nanopaper, and to reported data of nonstretched NFC/HEC nanocomposite of similar composition (wt % NFC = 68; wt % HEC = 32, see ref 19).

As for the TEMPO-NFC nanopaper, the TEMPO-NFC/HEC nanocomposites have higher modulus, strength and lower strain to failure than the nondrawn composites. Interestingly, even at their highest draw-ratio, the nanocomposites have a relatively high strain to failure of 6.1%. The strength and modulus of the nanocomposite are considerably higher than those of nondrawn composite samples (modulus of 13.3 GPa and strength of 355 MPa for drawn composite vs modulus of 8.2 GPa and strength of 200 MPa for nondrawn composite). Properties are also improved compared wtih nondrawn nanopaper. The work to fracture (area under the stress−strain curves) of the drawn nanocomposites is greater than that of drawn and nondrawn TEMPO-NFC nanopaper. Cold drawing of the TEMPO-NFC/HEC nanocomposites is an alternative to cold drawing of TEMPO-NFC nanopaper, permitting an increase in the strength without compromising strain to failure and toughness.

CONCLUSION

An environmentally friendly process was developed for cold drawing of wet TEMPO-NFC hydrogels with 70−90% water, followed by drying. Optically transparent nanopaper based on oriented TEMPO-NFC nanofibers is obtained. This process does not rely on harmful solvents, is carried out at room temperature and utilizes TEMPO-NFC nanofibers extracted from wood pulp fibers. The draw-ratio correlated with degree of cellulose orientation and this in turn correlated with modulus in the draw direction. Maximum modulus was 33 GPa and maximum strength in tension was 430 MPa. This indicates the potential of drawn TEMPO-NFC nanopaper as tapes or laminae in laminated composites, where the directional dependence of mechanical properties can be tailored. Furthermore, AFM data as well as modulus data indicate that TEMPO-NFC in nanopaper can be oriented to a larger extent. Improved understanding of the orientation process itself is therefore desirable. Also the data on TEMPO-NFC/HEC combinations show that addition of polymer can have beneficial effects on the structure and properties of the oriented material. The present study indicates that TEMPO-NFC films oriented by cold drawing of hydrogel structures have interesting structure and mechanical properties, and deserve to be studied further. This is justified in terms of potential applications and in the improved understanding of structure−property relationships it will generate. This includes the strength potential of TEMPO-NFC films.

AUTHOR INFORMATION

Corresponding Author

*Tel.: +46-8-7908037. Fax: +46-8-7906166. E-mail: houssine@kth.se.

Notes

The authors declare no competing financial interest.

ACKNOWLEDGMENTS

N. E. Mushi is funded by Formas in the Carbomat center at KTH.

REFERENCES

(1) Turbak, A. F.; Snyder, F. W.; Sandberg, K. R. *J. Appl. Polym. Sci., Part A* **1983**, *37*, 815−827.

(2) Henriksson, M.; Henriksson, G.; Berglund, L. A.; Lindstrom, T. *Eur. Polym. J.* **2007**, *43*, 3434−3441.

(3) Paakko, M.; Ankerfors, M.; Kosonen, H.; Nykanen, A.; Ahola, S.; Osterberg, M.; Ruokolainen, J.; Laine, J.; Larsson, P. T.; Ikkala, O.; Lindstrom, T. *Biomacromolecules* **2007**, *8*, 1934−1941.

(4) Saito, T.; Nishiyama, Y.; Putaux, J. L.; Vignon, M.; Isogai, A. *Biomacromolecules* **2006**, *7*, 1687−1691.

(5) Henriksson, M.; Berglund, L. A.; Isaksson, P.; Lindstrom, T.; Nishino, T. *Biomacromolecules* **2008**, *9*, 1579−1585.
(6) Spence, K.; Venditti, R.; Rojas, O.; Habibi, Y.; Pawlak, J., Large-Scale Production of Biodegradable Plastics Using Energy Efficient Processes. In *Microfluidics Webinar*.
(7) Taniguchi, T.; Okamura, K. *Polym. Int.* **1998**, *47*, 291−294.
(8) Saito, T.; Kimura, S.; Nishiyama, Y.; Isogai, A. *Biomacromolecules* **2007**, *8*, 2485−2491.
(9) Chen, W.; Yu, H.; Liu, Y.; Chen, P.; Zhang, M.; Hai, Y. *Carbohydr. Polym.* **2011**, *83*, 1804−1811.
(10) Iwamoto, S.; Kai, W. H.; Isogai, A.; Iwata, T. *Biomacromolecules* **2009**, *10*, 2571−2576.
(11) Sehaqui, H. Nanofiber networks, aerogels and biocomposites based on nanofibrillated cellulose from wood. *PhD thesis*, Royal Institute of Technology, Stockhold, Sweden, 2011.
(12) Sehaqui, H.; Liu, A. D.; Zhou, Q.; Berglund, L. A. *Biomacromolecules* **2010**, *11*, 2195−2198.
(13) Svagan, A. J.; Samir, M.; Berglund, L. A. *Adv. Mater.* **2008**, *20*, 1263−1269.
(14) Sehaqui, H.; Salajkova, M.; Zhou, Q.; Berglund, L. A. *Soft Matter* **2010**, *6*, 1824−1832.
(15) Paakko, M.; Vapaavuori, J.; Silvennoinen, R.; Kosonen, H.; Ankerfors, M.; Lindstrom, T.; Berglund, L. A.; Ikkala, O. *Soft Matter* **2008**, *4*, 2492−2499.
(16) Sehaqui, H.; Zhou, Q.; Berglund, L. A. *Compos. Sci. Technol.* **2011**, *71*, 1593−1599.
(17) Zimmermann, T.; Pohler, E.; Geiger, T. *Adv. Eng. Mater.* **2004**, *6*, 754−761.
(18) Bruce, D. M.; Hobson, R. N.; Farrent, J. W.; Hepworth, D. G. *Compos., A* **2005**, *36*, 1486−1493.
(19) Sehaqui, H.; Zhou, Q.; Berglund, L. A. *Soft Matter* **2011**, *7*, 7342−7350.
(20) Nystrom, G.; Razaq, A.; Stromme, M.; Nyholm, L.; Mihranyan, A. *Nano Lett.* **2009**, *9*, 3635−3639.
(21) Olsson, R. T.; Azizi Samir, M. A. S.; Salazar-Alvarez, G.; Belova, L.; Ström, V.; Berglund, L. A.; Ikkala, O.; Nogués, J.; Gedde, U. W. *Nat. Nanotechnol.* **2010**, *5*, 584−588.
(22) Yano, H.; Sugiyama, J.; Nakagaito, A. N.; Nogi, M.; Matsuura, T.; Hikita, M.; Handa, K. *Adv. Mater.* **2005**, *17*, 153−155.
(23) Revol, J. F.; Bradford, H.; Giasson, J.; Marchessault, R. H.; Gray, D. G. *Int. J. Biol. Macromol.* **1992**, *14*, 170−172.
(24) Sugiyama, J.; Chanzy, H.; Maret, G. *Macromolecules* **1992**, *25*, 4232−4234.
(25) Bordel, D.; Putaux, J. L.; Heux, L. *Langmuir* **2006**, *22*, 4899−4901.
(26) Nishiyama, Y.; Kuga, S.; Wada, M.; Okano, T. *Macromolecules* **1997**, *30*, 6395−6397.
(27) Gindl, W.; Keckes, J. *J. Appl. Polym. Sci.* **2007**, *103*, 2703−2708.
(28) Iwamoto, S.; Isogai, A.; Iwata, T. *Biomacromolecules* **2011**, *12*, 831−836.
(29) Uddin, A. J.; Araki, J.; Gotoh, Y. *Biomacromolecules* **2011**, *12*, 617−624.
(30) Olsson, R. T.; Kraemer, R.; Lopez-Rubio, A.; Torres-Giner, S.; Jose Ocio, M.; Maria Lagaron, J. *Macromolecules* **2010**, *43*, 4201−4209.
(31) Nogi, M.; Iwamoto, S.; Nakagaito, A. N.; Yano, H. *Adv. Mater.* **2009**, *21*, 1595-+.
(32) Liu, A.; Walther, A.; Ikkala, O.; Belova, L.; Berglund, L. A. *Biomacromolecules* **2011**, *12*, 633−641.
(33) Nishino, T.; Takano, K.; Nakamae, K. *J. Polym. Sci., B* **1995**, *33*, 1647−1651.
(34) Nakagaito, A. N.; Yano, H. *Appl. Phys. A: Mater. Sci. Process.* **2004**, *78*, 547−552.
(35) Gindl, A. W.; Veigel, S.; Kekces, J., Cellulosic nanomaterials with preferred orientation. Salmen, L (Ed). Novel materials from wood cellulose. In *Annual meeting of IAWS*; Innventia AB: Stockholm, Sweden, 2011; p 90.
(36) Sehaqui, H.; Berglund, L. A.; Zhou, Q. *Biomacromolecules* **2011**, *12*, 3638−3644.
(37) Syverud, K.; Stenius, P. *Cellulose* **2009**, *16*, 75−85.